Narrow escape with imperfect reactions

Anıl Cengiz [*] and Sean D. Lawley [†]

Department of Mathematics, University of Utah, Salt Lake City, Utah 84112, USA

The imperfect narrow escape problem considers the mean first passage time (MFPT) of a Brownian particle through one of several small, partially reactive traps on an otherwise reflecting boundary within a confining domain. Mathematically, this problem is equivalent to Poisson's equation with mixed Neumann-Robin boundary conditions. Here, we obtain this MFPT in general three-dimensional domains by using strong localized perturbation theory in the small trap limit. These leading-order results involve factors, which are analogous to electrostatic capacitances, and we use Brownian local time theory and kinetic Monte Carlo (KMC) algorithms to rapidly compute these factors. Furthermore, we use a heuristic approximation of such a capacitance to obtain a simple, approximate MFPT, which is valid for any trap reactivity. In addition, we develop KMC algorithms to efficiently simulate the full problem and find excellent agreement with our asymptotic approximations.

I. INTRODUCTION

The narrow escape problem, first posed by Rayleigh [1], refers to the escape time of a Brownian particle confined in a bounded domain whose boundary is reflecting except for some number of small absorbing windows (traps) through which the particle can escape. This problem is of particular interest in cell biology as ions, neurotransmitters, and substrate molecules have all been modeled as Brownian particles looking to bind small targets such as protein channels, receptors, or enzymes on a cell membrane [2,3]. In these diverse biophysical scenarios, the timescales of critical intracellular processes are thus governed by the time it takes a diffusing particle to find a small target.

There have been extensive studies on the narrow escape problem in two-dimensional and three-dimensional domains in the case of "perfect" absorption, i.e., when the Brownian particle gets absorbed immediately upon first contact with a trap. In the small trap limit, the leading-order asymptotic behavior of the mean first passage time (MFPT) of exit in arbitrary domains and the higher-order terms in select geometries have been derived for systems with perfectly absorbing traps [3–8]. However, targets like protein channels or receptors/enzymes may often be better modeled as having finite reactivity, since the particles may not always be captured shortly after their first encounter with the traps [9]. Orientational constraints on the diffusing particles [10] and energetic activation barriers for the traps [11] might require the diffusing particle to make multiple visits to the trap before getting absorbed. The so-called "imperfect" narrow escape problem arises in such cases [12] and currently has fewer available results compared to the perfect narrow escape problem. In the limit of large domain volume, this imperfect narrow escape

problem was studied in Ref. [13] in three dimensions and in Ref. [12] in two and three dimensions. The kinetics of imperfect reactions have been investigated in Refs. [14–17] for particular geometries in cylindrical and spherical domains exploiting domain-dependent eigenfunctions and the uniform flux approximation. Diffusion to partially absorbing traps has also been studied in the context of boundary homogenization [18,19]. Other aspects of diffusion-controlled reactions with finite reactivity were also discussed in [20,21].

In this paper, we derive the leading-order asymptotic behavior of the MFPT in imperfect narrow escape problems in three-dimensional domains of arbitrary geometry. We use the method of strong localized perturbation theory (SLPT) [5,6,22,23] to estimate the MFPT in the limit of vanishing trap size. To briefly summarize our main results, suppose the Brownian particle diffuses with diffusivity $D > 0$ in a bounded, three-dimensional domain $\Omega \subset \mathbb{R}^3$ with volume $|\Omega|$. The boundary is reflecting except for $N \geqslant 1$ small, well-separated, locally circular traps with common permeability $\tilde{\kappa} > 0$. The traps have radii $a_1, \ldots, a_N$ with $a_i/a_n = O(1)$ and average radius much less than the lengthscale of the confining domain,

$$a := \frac{1}{N} \sum_{n=1}^{N} a_n \ll |\Omega|^{1/3}. \tag{1}$$

Denoting the MFPT by v and assuming that the Brownian particle does not start near a trap, we obtain the following asymptotic behavior of the MFPT in the small trap limit in (1):

$$v \sim \begin{cases} \dfrac{|\Omega|}{4DNa} & \text{if } a\tilde{\kappa}/D \gg 1, \\[2ex] \dfrac{|\Omega|}{2\pi D \sum_{n=1}^{N} a_n c_2(1, a_n \tilde{\kappa}/D)} & \text{if } a\tilde{\kappa}/D = O(1), \\[2ex] \dfrac{|\Omega|}{2\pi K\tilde{\kappa} \sum_{n=1}^{N} a_n^2} & \text{if } a\tilde{\kappa}/D \ll 1, \end{cases} \tag{2}$$

where $c_2(1, a_n \tilde{\kappa}/D)$ is analogous to the electrostatic capacitance of a unit disk with dimensionless permeability

─────────
[*]Contact author: cengiz@math.utah.edu
[†]Contact author: lawley@math.utah.edu

$a_n \tilde{\kappa}/D$ and $K \approx 0.5854$ is analogous to the electrostatic capacitance of a unit disk with a fixed unit flux (see Sec. II for details). While we do not have an exact formula for the function c_2 or the constant K, we use a kinetic Monte Carlo (KMC) algorithm to rapidly compute these factors.

Furthermore, using a previously posited heuristic formula for c_2 [19] and assuming that all the traps are the same size (i.e., $a_i = a$ for $i = 1, \ldots, N$), we find that the MFPT is well approximated in the small trap limit in (1) by

$$v \approx \frac{|\Omega|}{4DNa}\left(1 + \frac{2}{K\pi}\frac{D}{a\tilde{\kappa}}\right), \tag{3}$$

where we again have $K \approx 0.5854$. Notice that (3) agrees with (2) in both the $a\tilde{\kappa}/D \gg 1$ regime (high absorption) and the $a\tilde{\kappa}/D \ll 1$ regime (low absorption). Furthermore, we show that the estimate (3) differs from (2) by no more than 5% regardless of the value of $a\tilde{\kappa}/D$. We emphasize that (3) is valid for any trap arrangement, provided the traps are well separated.

The result in (3) has a simple interpretation. The first term in (3) is the MFPT in the case of perfectly absorbing traps [8] and thus represents the time for the particle to first hit the trap. The second term in (3) assumes that the particle starts on the trap and accounts for the additional time to be absorbed that stems from the finite-trap permeability.

The rest of the paper is structured as follows. In Sec. II, we formulate the imperfect narrow escape problem and use the method of SLPT to treat the problem in the three separate absorption regimes in (2). We derive expressions for the MFPT in all three regimes as a function of the trap permeability and the capacitance of the corresponding generalized electrified disk problem, which can be rapidly computed by KMC algorithms or approximated via prior estimates [19]. In Sec. III, we compare our analytical results on the MFPT to numerical results obtained by KMC simulations of the full stochastic system. We also discuss how this framework allows us to observe the scaling law recently proposed by Guérin *et al.* (2023) for a particle starting at the boundary of a partially absorbing trap [12]. In Sec. IV, we describe the KMC algorithms used to compute the capacitance of the required electrified disk problems and to simulate the full problem in the case of a three-dimensional rectangular domain with a single, partially absorbing trap. These KMC algorithms break down the Brownian search process into subprocesses whose probability distributions are well characterized [19,24]. We conclude in Sec. V by discussing the implications and limitations of our paper. The Appendices collect some technical points of the analysis and the numerical algorithms.

II. MATHEMATICAL ANALYSIS

A. Problem formulation

Consider a Brownian particle diffusing in a bounded, three-dimensional domain $\Omega \subset \mathbb{R}^3$. Suppose the boundary $\partial\Omega$ is smooth and consists of a reflective portion $\partial\Omega_R$ and $N \geqslant 1$ small traps $\partial\Omega_A = \cup_{n=1}^N \partial\Omega_n$ so that $\partial\Omega = \partial\Omega_R \cup \partial\Omega_A$. Assume that the traps are partially absorbing, locally circular, and centered at $\mathbf{x}_n \in \partial\Omega$ with radius a_n for $n = 1, \ldots, N$. Define the MFPT $v(x)$ as the expected time taken by the

Brownian particle starting at $x \in \Omega$ to exit the domain through one of the traps. Denoting the diffusivity of the particle by D and the "permeability" (or "reactivity" or "trapping rate") of the traps by $\tilde{\kappa}$, the MFPT $v(x)$ satisfies the following Poisson equation with mixed Robin-Neumann boundary conditions [25]:

$$D\Delta v = -1, \quad \mathbf{x} \in \Omega,$$
$$D\partial_n v = \begin{cases} 0, & \mathbf{x} \in \partial\Omega_R, \\ -\tilde{\kappa}v, & \mathbf{x} \in \partial\Omega_A, \end{cases} \tag{4}$$

where ∂_n denotes the normal derivative.

To simplify the analysis, we nondimensionalize the problem by rescaling space by L and rescaling time by L^2/D [i.e., $\mathbf{x} \to \mathbf{x}/L$ and $t \to t/(L^2/D)$], where

$$L := |\Omega|^{1/3}$$

denotes the characteristic lengthscale of the domain. The dimensionless problem thus has unit diffusivity in a domain of unit volume and the traps have average radius

$$\varepsilon := \frac{a}{L} = \frac{\frac{1}{N}\sum_{n=1}^N a_n}{L}$$

and dimensionless permeability

$$\kappa := \frac{\tilde{\kappa}L}{D}.$$

The dimensionless problem is then described by

$$\Delta v = -1, \quad \mathbf{x} \in \Omega,$$
$$\partial_n v = \begin{cases} 0, & \mathbf{x} \in \partial\Omega_R, \\ -\kappa v, & \mathbf{x} \in \partial\Omega_A. \end{cases} \tag{5}$$

For simplicity, we use Ω to denote both the dimensional and dimensionless domain (and similarly for $\partial\Omega$, $\partial\Omega_R$, $\partial\Omega_A$, and $\partial\Omega_n$). We also sometimes retain $|\Omega|$ in formulas below even though this volume has been set to unity in our nondimensionalization.

Below, we use SLPT to study the MFPT in the small trap limit of $\varepsilon \ll 1$. We assume that the absorbing traps are well separated in the sense that

$$\|\mathbf{x}_n - \mathbf{x}_m\| = O(1), \quad \text{if } n \neq m,$$

and that the traps have similar sizes, i.e., $a_n/a = O(1)$ for $n = 1, \ldots, N$.

B. Strong localized perturbation analysis

The method of SLPT involves matching an outer solution to an inner solution around a trap. The series expansion for the outer solution depends on the relative size of the trap and its permeability. Therefore, we treat this problem in three separate absorption regimes: Case 1: $\kappa\varepsilon \gg 1$ (high absorption), Case 2: $\kappa\varepsilon = O(1)$ (medium absorption), and Case 3: $\kappa\varepsilon \ll 1$ (low absorption).

1. Case 1: $\kappa\varepsilon \gg 1$

In the outer region away from an $O(\varepsilon)$ neighborhood of any trap, we expand the outer solution to (5) as

$$v \sim \varepsilon^{-1}v_0 + v_1 + \text{h.o.t.}, \tag{6}$$

where h.o.t. represents higher-order terms. Here, v_0 is an unknown constant, and v_1 is a function to be determined. Substituting (6) into (5) and matching the $O(1)$ terms yields

$$\Delta v_1 = -1, \quad \mathbf{x} \in \Omega, \tag{7}$$

$$\partial_n v_1 = 0, \quad \mathbf{x} \in \partial\Omega \setminus \{\mathbf{x}_1, \ldots, \mathbf{x}_N\}. \tag{8}$$

Notice that from the perspective of the outer solution, the traps have shrunk to points.

In the inner region near the nth trap, we introduce the local variables,

$$\mathbf{y} := \varepsilon^{-1}(\mathbf{x} - \mathbf{x}_n), \quad w(\mathbf{y}) := v(\mathbf{x}_n + \varepsilon\mathbf{y}), \tag{9}$$

and pose the following inner expansion:

$$w \sim \varepsilon^{-1} w_0 + \text{h.o.t.} \tag{10}$$

We denote the magnified trap, which is a disk of radius

$$\alpha_n := a_n/a,$$

by $\partial\Omega_{A,0} = \varepsilon^{-1}\partial\Omega_n$, the magnified reflective region as $\partial\Omega_{R,0}$ and the magnified domain (half of three-dimensional space) as $\partial\Omega_0$. Applying the Laplacian with respect to $\mathbf{y}$ to w and using (5) yields $\Delta_\mathbf{y} w = \varepsilon^2 \Delta w = -\varepsilon^2$. Then, applying $\Delta_\mathbf{y}$ on the inner expansion in (10), we obtain the following problem:

$$\Delta_\mathbf{y} w_0 = 0, \quad \mathbf{y} \in \Omega_0,$$

$$\partial_n w_0 = \begin{cases} 0, & \mathbf{y} \in \partial\Omega_{R,0}, \\ -\varepsilon\kappa w_0, & \mathbf{y} \in \partial\Omega_{A,0}. \end{cases} \tag{11}$$

The matching condition ensures that the near-field behavior of the outer solution as $\mathbf{x} \to \mathbf{x}_n$ agrees with the far-field behavior of the inner solution as $\|\mathbf{y}\| \to \infty$,

$$\varepsilon^{-1} v_0 + v_1 + \text{h.o.t.} \sim \varepsilon^{-1} w_0 + \text{h.o.t.} \tag{12}$$

Matching the $O(\varepsilon^{-1})$ terms imposes that $v_0 \sim w_0$ as $\|\mathbf{y}\| \to \infty$. Define a function w_c by

$$w_0 = v_0(1 - w_c). \tag{13}$$

It follows that w_c must satisfy

$$\Delta_\mathbf{y} w_c = 0, \quad \mathbf{y} \in \Omega_0,$$

$$\partial_n w_c = 0, \quad \mathbf{y} \in \partial\Omega_{R,0},$$

$$w_c = 1, \quad \mathbf{y} \in \partial\Omega_{A,0},$$

$$w_c \to 0, \quad \text{as } \|\mathbf{y}\| \to \infty. \tag{14}$$

To derive the boundary conditions in (14), differentiate (13) and use (11) to obtain

$$\partial_n w_c = \frac{-1}{v_0} \partial_n w_0$$

$$= \frac{-1}{v_0} \begin{cases} -\varepsilon\kappa w_0, & \mathbf{y} \in \partial\Omega_{A,0}, \\ 0, & \mathbf{y} \in \partial\Omega_{R,0}, \end{cases}$$

$$= \begin{cases} \varepsilon\kappa(1 - w_c), & \mathbf{y} \in \partial\Omega_{A,0}, \\ 0, & \mathbf{y} \in \partial\Omega_{R,0}. \end{cases} \tag{15}$$

Taking $\varepsilon\kappa \to \infty$ gives the boundary conditions in (14) for Case 1 ($\varepsilon\kappa \gg 1$).

The problem in (14) is the so-called electrified disk problem in electrostatics [26]. The far-field behavior of the

solution has the following form:

$$w_c \sim \frac{c_1(\alpha_n)}{\|\mathbf{y}\|} + O(\|\mathbf{y}\|^{-2}) \quad \text{as } \|\mathbf{y}\| \to \infty, \tag{16}$$

where we refer to the constant $c_1(\alpha_n)$ as the capacitance. The subscript 1 denotes that this is for Case 1, and α_n is the radius of the disk $\partial\Omega_{A,0}$. It is well known that the capacitance for the electrified disk problem is [7]

$$c_1(r) = 2r/\pi, \quad \text{for all } r > 0.$$

The far-field behavior in (16), the relation (15), and the matching condition (12) yield the following singularity condition on v_1:

$$v_1 \sim -\frac{v_0 c_1(\alpha_n)}{\|\mathbf{x} - \mathbf{x}_n\|} \quad \text{as } \mathbf{x} \to \mathbf{x}_n. \tag{17}$$

The problem for v_1 in (7) and (8) and the singular behavior in (17) can be written in distributional form as

$$\Delta v_1 = -1, \quad \mathbf{x} \in \Omega,$$

$$\partial_n v_1 = -\sum_{n=1}^{N} 2\pi v_0 c_1(\alpha_n)\delta(\mathbf{x} - \mathbf{x}_n), \quad \mathbf{x} \in \partial\Omega. \tag{18}$$

Integrating Poisson's equation in (18) and using the divergence theorem implies that

$$v_0 = \frac{|\Omega|}{2\pi \sum_{n=1}^{N} c_1(\alpha_n)}. \tag{19}$$

Recalling the expansion (6), the leading-order behavior of the MFPT in (5) when $\kappa\varepsilon \gg 1$ is thus given by

$$v \sim \frac{|\Omega|}{2\pi\varepsilon \sum_{n=1}^{N} c_1(\alpha_n)} = \frac{|\Omega|}{4\varepsilon \sum_{n=1}^{N} \alpha_n} \quad \text{as } \varepsilon \to 0.$$

We can dimensionalize this MFPT expression to write the MFPT solution to the dimensional problem in (4) in the $a\tilde{\kappa}/D \gg 1$ regime as

$$v \sim \frac{|\Omega|}{4DNa} \quad \text{as } \frac{a}{L} \to 0. \tag{20}$$

Naturally, (20) reproduces the MFPT in the case of perfectly absorbing traps [8].

Observe that (20) can be written as

$$v \sim 1 \bigg/ \left(\sum_{n=1}^{N} 1/v^{(n)}\right) \quad \text{as } \frac{a}{L} \to 0, \tag{21}$$

if we define

$$v^{(n)} := \frac{|\Omega|}{4Da_n}$$

is the asymptotic MFPT to absorption by the nth trap (ignoring other traps). That is, Nv is the harmonic mean of the MFPTs to each of the N traps, which is reminiscent of the parallel connection of resistances in electrostatics.

2. Case 2: $\kappa\varepsilon = O(1)$

The analysis of Case 2 ($\varepsilon\kappa = O(1)$) proceeds along identical lines as Case 1 ($\varepsilon\kappa \gg 1$), except the problem (14) is

replaced by

$$\Delta_{\mathbf{y}} w_c = 0, \quad \mathbf{y} \in \Omega_0,$$
$$\partial_n w_c = 0, \quad \mathbf{y} \in \partial\Omega_{R,0},$$
$$\partial_n w_c = \varepsilon\kappa(1 - w_c), \quad \mathbf{y} \in \partial\Omega_{A,0},$$
$$w_c \to 0, \quad \text{as } \|\mathbf{y}\| \to \infty. \tag{22}$$

By analogy to (14), we refer to (23) as a "generalized electrified disk problem." Note that the boundary conditions in (23) follows immediately from (15).

Similar to (16), the far-field behavior of the solution to (23) has the following form:

$$w_c \sim \frac{c_2(\alpha_n, \varepsilon\kappa)}{\|\mathbf{y}\|} + O(\|\mathbf{y}\|^{-2}) \text{ as } \|\mathbf{y}\| \to \infty,$$

where we refer to the constant $c_2(\alpha_n, \varepsilon\kappa)$ as the capacitance. We note that similar far-field behavior of certain PDE solutions was also found in [12,13]. Notice that c_2 is a function of the radius α_n of the disk $\partial\Omega_{A,0}$ and the permeability $\varepsilon\kappa$ appearing in (23). Below, we show how to either compute this capacitance using a KMC algorithm or approximate its value using a simple heuristic formula.

Proceeding along identical lines as in Case 1, except replacing $c_1(\alpha_n)$ by $c_2(\alpha_n, \varepsilon\kappa)$, yields the following leading-order behavior of the MFPT in (5) when $\kappa\varepsilon = O(1)$:

$$v \sim \frac{|\Omega|}{2\pi\varepsilon \sum_{n=1}^{N} c_2(\alpha_n, \varepsilon\kappa)} \text{ as } \varepsilon \to 0.$$

We can dimensionalize this MFPT expression to write the MFPT solution to the dimensional problem in (4) in the $a\tilde{\kappa}/D = O(1)$ regime as

$$v \sim \frac{|\Omega|}{2\pi D \sum_{n=1}^{N} a_n c_2(1, a_n\tilde{\kappa}/D)} \text{ as } \frac{a}{L} \to 0. \tag{23}$$

Observe that (23) implies that (21) holds if we define the asymptotic MFPT to the nth trap (ignoring other traps),

$$v^{(n)} := \frac{|\Omega|}{2\pi D a_n c_2(1, a_n\tilde{\kappa}/D)}.$$

3. Case 3: $\kappa\varepsilon \ll 1$

To handle Case 3 ($\kappa\varepsilon \ll 1$), we assume that

$$\kappa = \varepsilon^s, \quad \text{for some } s > -1.$$

In the outer region away from an $O(\varepsilon)$ neighborhood of $\mathbf{x}_n$, we expand the outer solution as

$$v \sim \varepsilon^{-s-2} v_0 + v_1 + \text{h.o.t.} \tag{24}$$

Here, v_0 is an unknown constant and v_1 is a function to be determined. Substituting (24) into (5) and matching the $O(1)$ terms, we again obtain the outer problem in (7) and (8).

In the inner region near the nth trap, we use the local variables in (9) and pose the following inner expansion:

$$v \sim \varepsilon^{-s-2} w_0 + \text{h.o.t.} \tag{25}$$

Using the relationship $\Delta_{\mathbf{y}} w = -\varepsilon^2$ and the inner expansion in (25), we obtain the problem in (11). The matching condition ensures that the near-field behavior of the outer solution as

$\mathbf{x} \to \mathbf{x}_n$ must agree with the far-field behavior of the inner solution as $\|\mathbf{y}\| \to \infty$,

$$\varepsilon^{-s-2} v_0 + v_1 + \text{h.o.t.} \sim \varepsilon^{-s-2} w_0 + \text{h.o.t.} \tag{26}$$

The matching condition on the $O(\varepsilon^{-s-2})$ terms imposes that $v_0 \sim w_0$ as $\|\mathbf{y}\| \to \infty$. Define a function w_c by

$$w_0 = v_0(1 - \varepsilon\kappa w_c). \tag{27}$$

It follows that w_c must satisfy

$$\Delta_{\mathbf{y}} w_c = 0, \quad \mathbf{y} \in \Omega_0,$$
$$\partial_n w_c = 0, \quad \mathbf{y} \in \partial\Omega_{R,0},$$
$$\partial_n w_c = 1, \quad \mathbf{y} \in \partial\Omega_{A,0},$$
$$w_c \to 0, \quad \text{as } \|\mathbf{y}\| \to \infty. \tag{28}$$

To derive the boundary conditions in (28), differentiate (27) and use (11) to obtain

$$\partial_n w_c = \frac{-1}{\varepsilon\kappa v_0} \partial_n w_0$$
$$= \frac{-1}{\varepsilon\kappa v_0} \begin{cases} 0, & \mathbf{y} \in \partial\Omega_{R,0}, \\ -\varepsilon\kappa w_0, & \mathbf{y} \in \partial\Omega_{A,0}, \end{cases}$$
$$= \begin{cases} 0, & \mathbf{y} \in \partial\Omega_{R,0}, \\ 1 - \varepsilon\kappa w_c, & \mathbf{y} \in \partial\Omega_{A,0}. \end{cases}$$

Taking $\varepsilon\kappa \to 0$ yields the boundary conditions in (28).

Similar to (16), the far-field behavior of the solution to (28) has the following form:

$$w_c \sim \frac{c_3(\alpha_n)}{\|\mathbf{y}\|} + O(\|\mathbf{y}\|^{-2}) \text{ as } \|\mathbf{y}\| \to \infty,$$

where we refer to the constant $c_3(\alpha_n)$ as the capacitance of the generalized electrified disk problem in (28). In this case, the capacitance is (see the Appendix C or Ref. [19])

$$c_3(\alpha_n) = \alpha_n^2 K, \tag{29}$$

where K depends on the expected local time of a Brownian particle on a unit disk and is documented to be $K \approx 0.5854$ [19].

Matching the $O(1)$ terms (26) yields the singularity condition in (17) with c_3 replacing c_1. Again writing this singularity condition in the distributional form in (18) and using the divergence theorem yields the formula for v_0 in (18) (with c_3 replacing c_1). The constant K in (29) can be computed to an arbitrary accuracy using the KMC algorithm discussed in Appendix C. The leading-order behavior of the MFPT in problem (5) when $\kappa\varepsilon \ll 1$ is thus given by

$$v \sim \frac{|\Omega|}{2\pi\varepsilon^2\kappa K \sum_{n=1}^{N} \alpha_n^2} \text{ as } \varepsilon \to 0.$$

We can dimensionalize this MFPT expression to write the MFPT solution to the dimensional problem in (4) in the $a\tilde{\kappa}/D \ll 1$ regime as

$$v \sim \frac{|\Omega|}{2\pi K\tilde{\kappa} \sum_{n=1}^{N} a_n^2} \text{ as } \frac{a}{L} \to 0. \tag{30}$$

TABLE I. Dimensionless MFPT asymptotics as $\varepsilon \to 0$ if the Brownian particle does not start in an $O(\varepsilon)$ neighborhood of any trap.

Parameter regime	Leading-order MFPT
Case 1: $\varepsilon \kappa \gg 1$ (high absorption)	$\dfrac{\lvert \Omega \rvert}{4\varepsilon \sum_{n=1}^{N} \alpha_n}$
Case 2: $\varepsilon \kappa = O(1)$ (medium absorption)	$\dfrac{\lvert \Omega \rvert}{2\pi \varepsilon \sum_{n=1}^{N} c_2(\alpha_n, \varepsilon \kappa)}$
Case 3: $\varepsilon \kappa \ll 1$ (low absorption)	$\dfrac{\lvert \Omega \rvert}{2\pi \varepsilon^2 K \kappa \sum_{n=1}^{N} \alpha_n^2}$

Observe that (30) implies that (21) holds if we define the asymptotic MFPT to the nth trap (ignoring other traps),

$$v^{(n)} := \frac{\lvert \Omega \rvert}{2\pi K \tilde{\kappa} a_n^2}.$$

C. A heuristic to combine the three cases

Our asymptotic estimates of the dimensionless MFPT for the three cases are reported in Table I. We emphasize that these MFPT results assume that the Brownian particle does not start in an $O(\varepsilon)$ neighborhood of any trap. Furthermore, these MFPT results also hold if the Brownian particle is initially uniformly distributed in the domain Ω, since the probability that a particle starts in an $O(\varepsilon)$ neighborhood of any trap is $O(\varepsilon)$ in this uniform case.

There are two limitations, which makes the results in Table I cumbersome to use. First, Table I shows that depending on the relative sizes of ε and κ, the asymptotic behavior of the MFPT is described by different expressions. Second, we do not have an exact formula for the capacitance $c_2(\alpha_n, \varepsilon \kappa)$ appearing in Case 2 [$\varepsilon \kappa = O(1)$, i.e., medium absorption]. We now present a heuristic estimate of c_2 to ameliorate both of these problems.

The capacitance c_2 can be computed using a KMC algorithm (detailed below). The following heuristic, sigmoidal estimate of c_2 was first posited in [19],

$$c_{\text{sig}}(\kappa') := \frac{(2/\pi)\kappa'}{\kappa' + 2/(\pi K)} \approx c_2(1, \kappa'), \tag{31}$$

where $K \approx 0.5854$ is the constant appearing in Case 3. The simple estimate (31) is quite accurate. Indeed, the relative error between $c_2(1, \kappa')$ and $c_{\text{sig}}(\kappa')$ is always less than 5%,

$$\frac{\lvert c_2(1, \kappa') - c_{\text{sig}}(\kappa') \rvert}{c_2(1, \kappa')} \leqslant 5\%, \tag{32}$$

and the maximum relative occurs for $\kappa' \approx 1$ (see Fig. 3 in [19]). Note that it is enough to consider $c_2(1, \kappa')$ as a function only of its second argument (here, denoted $\kappa' > 0$) since a simple scaling argument applied to (23) shows that

$$c_2(r, \kappa') = l c_2(r/l, l\kappa'), \quad \text{for all } r, \kappa', l > 0. \tag{33}$$

Using the scaling (33) and the sigmoidal estimate in (31) for Case 2 yields the following estimate of the dimensionless MFPT:

$$v \approx \left(\sum_{n=1}^{N} 1/v_n \right)^{-1}, \quad \text{where } v_n = \frac{\lvert \Omega \rvert}{4\alpha_n \varepsilon} \left(1 + \frac{2}{\pi K \alpha_n \varepsilon \kappa} \right). \tag{34}$$

When $\varepsilon \kappa = O(1)$, the expression in (34) approximates the expression the MFPT for Case 2 in Table I using the capacitance approximation in (31). Furthermore, notice that (34) reduces to the expressions in Table I for Case 1 and Case 3 in the respective regimes of $\varepsilon \kappa \gg 1$ and $\varepsilon \kappa \ll 1$. Summarizing, the single, analytical expression in (34) approximates the MFPT for all three cases. In addition, it follows from the error bound in (32) that the expression (34) never deviates from the expressions in Table I by more than 5%.

If all the traps have the same size (i.e., $\alpha_n = 1$ for $n = 1, \ldots, N$), then the expression in (34) simplifies to

$$v \approx \frac{1}{N} \frac{\lvert \Omega \rvert}{4\varepsilon} \left(1 + \frac{2}{\pi K \varepsilon \kappa} \right). \tag{35}$$

The result in (35) has a simple interpretation. The first term is the MFPT in the case of perfectly absorbing traps [8] and thus represents the time for the particle to first hit the trap. The second term then accounts for the additional time to be absorbed that stems from the finite-trap permeability assuming that the particle starts on the trap.

III. COMPARISON TO NUMERICAL SIMULATIONS

In this section, we compare the analytical results derived in Sec. II to numerical simulations.

A. Full stochastic system

We compare the accuracy of the analytical asymptotic results in Table I to the numerical results that we generate by simulating the full imperfect narrow escape problem in (5). As we detail in Sec. IV below, we use KMC algorithms to rapidly simulate the full stochastic system. In these simulations, the domain is a rectangular prism defined by $\Omega = (-1, 1) \times (-1, 1) \times (0, \sqrt{2}) \subset \mathbb{R}^3$. There is $N = 1$ trap, and it is located at the "bottom" of the domain,

$$\partial \Omega_A = \partial \Omega_1 = \{(x, y, 0) \, : \, x^2 + y^2 < a^2\}.$$

In each simulation, the initial position of the Brownian particle is chosen randomly from a uniform distribution. As described in Sec. II, the MFPT results in Table I assume that the particle does not start in an $O(\varepsilon)$ neighborhood of any trap. However, the MFPT results in Table I still hold in the case of a particle that starts uniformly since there is merely an $O(\varepsilon)$ probability that such a uniformly distributed particle starts in an $O(\varepsilon)$ neighborhood of any trap. The trap radius ε and trap permeability κ are varied in the simulations to explore the dependence on trap radius and absorption regimes.

Figure 1 compares the analytical results derived using the method of SLPT to the numerical results obtained by KMC algorithms. In the figures, the relative errors of the analytical results never exceed 10%.
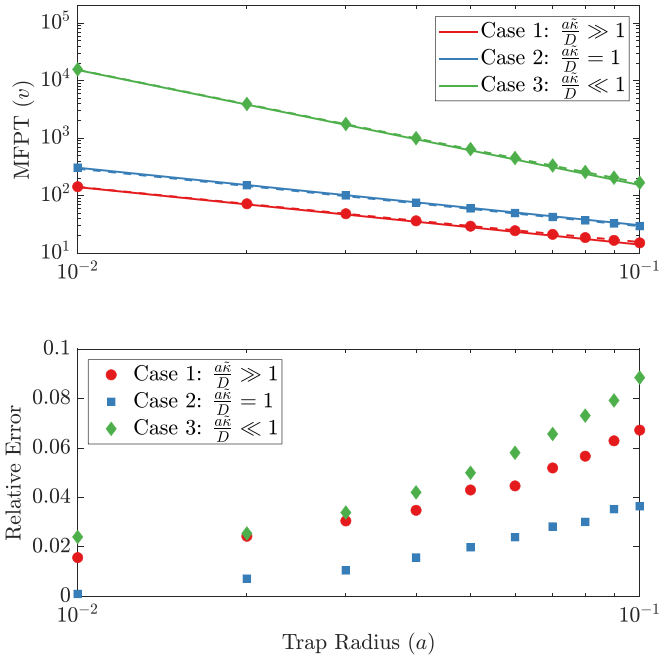
FIG. 1. SLPT Results vs KMC simulation Results. We compare the analytical results derived using the method of SLPT to the heuristic formula in (3) and the numerical results obtained by KMC simulations. The solid lines represent the asymptotic results, the dashed lines represent the heuristic result, and the markers represent the numerical results. We take $N = 1$, $D = 1$ for all cases, and $\tilde{\kappa} = 1/a^2$ in Case 1, $\tilde{\kappa} = 1/a$ in Case 2, and $\tilde{\kappa} = 1$ in Case 3.

B. Special case: Particles initialized at trap boundary

In the preceding subsection, we assumed that the Brownian particle was initially uniformly distributed in the domain. Guérin *et al.* [12] recently considered an interesting alternative scenario in which the particle starts at the boundary or "edge" of a partially reactive trap. In this case, their analysis found the following anomalous scaling for large reactivity and fixed $\varepsilon \ll 1$ (using the dimensionless problem of Sec. II):

$$v \sim \frac{|\Omega|}{2\varepsilon\sqrt{2\pi\kappa\varepsilon}} \quad \text{as } \kappa \to \infty. \tag{36}$$

We now use the matched asymptotic analysis of Sec. II and the KMC algorithms of Sec. IV to investigate (36).

The inner expansion in (10) describes the MFPT of a particle that starts near a trap. For simplicity, we follow [12] and assume that there is $N = 1$ trap, which is centered at $\mathbf{x}_1 \in \partial\Omega$. Hence, assuming that the particle starts at a point $\mathbf{x}_0$ near the "edge" of the trap, we use (10), (13), and (20) to approximate the MFPT for fixed $\varepsilon \ll 1$ and $\kappa \to \infty$ as

$$v(\mathbf{x}_0) \sim \frac{v_0}{\varepsilon}(1 - w_c(\mathbf{y}_0)) \sim \frac{|\Omega|}{4\varepsilon}(1 - w_c(\mathbf{y}_0)), \tag{37}$$

where w_c satisfies (23) and $\mathbf{y}_0 = (\mathbf{x}_0 - \mathbf{x}_1)/\varepsilon$. Therefore, we can estimate the MFPT for a particle initialized near the trap boundary by calculating $w_c(\mathbf{y}_0)$.

In Fig. 2, we plot the estimate in (37) for various initial trap locations using a KMC algorithm (detailed below) to calculate $w_c(\mathbf{y}_0)$. This plot shows excellent agreement with the result of Guérin *et al.* [12] in (36), and demonstrates how
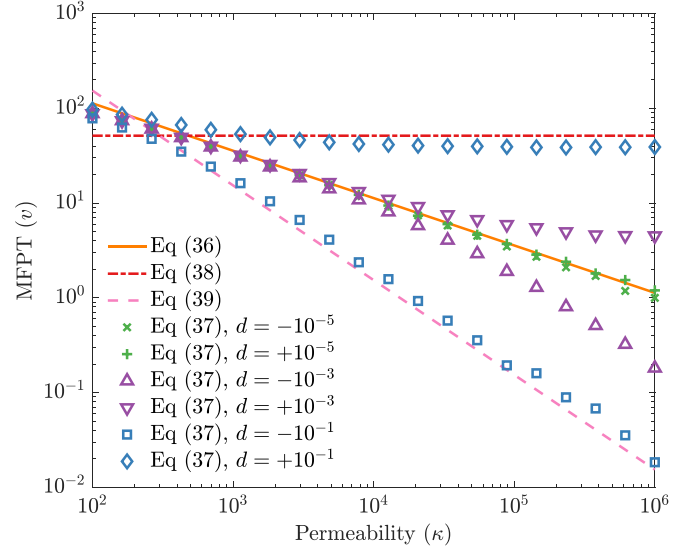

FIG. 2. SLPT results in (37) computed by KMC simulations agree with the formula in (36) from Guérin *et al.* (2023) [12] and approximations in (38) and (39) for particles that start near the trap boundary. The particle's initial position $\mathbf{y}_0$ is on the plane containing the trap (a unit disk) at a distance $d + 1$ from the center of the trap. In particular, $d > 0$ means the particle starts outside of the trap, and $d < 0$ means it starts on the trap. We take $\varepsilon = 10^{-2}$ and $|\Omega| = 4\sqrt{2}$.

the scaling deviates from (36) when the particle is initialized further from the "edge" of the trap. In particular, for the calculation of $w_c(\mathbf{y}_0)$, the trap is a partially absorbing unit disk with dimensionless reactivity $\varepsilon\kappa$ on an otherwise reflecting plane [recall that $w_c(\mathbf{y}_0)$ concerns the inner problem]. The markers in Fig. 2 are (37) with initial particle position $\mathbf{y}_0$ on the plane containing the trap, located at a distance $d + 1$ from the center of the trap. In particular, the green "x" ("+") markers are for $d = -10^{-5}$ ($d = +10^{-5}$), meaning that the particle starts on the inside (outside) edge of the trap. As expected, these green markers agree with the anomalous scaling in (36) found in [12]. However, Fig. 2 shows that the MFPT scaling deviates from (36) if the particle starts slightly further from the trap edge. Specifically, the deviation from (36) is noticeable for $\kappa \gtrsim 10^5$ when the initial position is $d = \pm 10^{-3}$ from the trap edge (purple triangle markers).

For $d = +10^{-1}$, the MFPT is roughly constant for large κ. This can be understood by noting that in this case, the FPT is dominated by the time required to first hit the trap (since large κ means it is quickly absorbed after hitting the trap), and this first hitting time is of course independent of κ. Further, for large κ and $d = +10^{-1}$, the probability of absorption $w_c(\mathbf{y}_0)$ is approximately the probability of eventually hitting the target, which is approximately the capacitance of a unit disk, $2/\pi$. Indeed, plugging $w_c(\mathbf{y}_0) \approx 2/\pi$ into (37) yields

$$v(\mathbf{x}_0) \sim \frac{|\Omega|}{4\varepsilon}(1 - 2/\pi), \tag{38}$$

which agrees reasonably well with the blue diamond markers.

For $d = -10^{-1}$, the blue square markers in Fig. 2 show that the MFPT in (37) agrees with the $1/\kappa$ scaling of

$$\frac{|\Omega|}{4\varepsilon}\frac{2}{K\pi\varepsilon\kappa}. \tag{39}$$

The estimate (39) is obtained from (35) by simply subtracting $|\Omega|/(4\varepsilon)$ (the time a particle takes to diffuse to the trap starting from the bulk) since the particle starts sufficiently far in the interior of the trap for $d = -10^{-1}$.

IV. KINETIC MONTE CARLO

In this section, we develop kinetic Monte Carlo (KMC) algorithms to run efficient particle-based simulations. These simulations compute the capacitance values shown in the analytical results and numerically simulate the MFPT in a particular domain geometry. These algorithms break down the diffusive search process into stages for which the associated probability distributions can be computed analytically. The basic idea of the methods dates back to the so-called walk-on-spheres method of Muller [27]. In this specific context, the methods are based on the KMC method devised by Bernoff, Lindsay, and Schmidt (2018) [24] and later developed in [19].

The algorithms for the capacitance problems and the full diffusion problem all rely on the same stages discussed below. For the capacitance problems, we take the domain to be half of three-dimensional space. For the MFPT simulation, we take the domain to be a rectangular prism, and we refer to the side of the prism that has the partially absorbing region as "the plane". The KMC algorithm breaks down the diffusive search process into three stages:

I. Project from bulk to plane. The particle starts away from the plane where it is free to diffuse, and it is propagated down to the plane. The time taken by the particle to first touch the plane and its location on the plane are drawn from exact probability distributions and recorded. The algorithm then proceeds to Stage II if the particle is outside of the absorbing region and to Stage III if the particle is inside the absorbing region.

II. Reflect off to space. The particle is on a reflective surface, and we propagate it to a hemisphere whose radius is the particle's distance to the trap boundary. The location of the particle on the hemisphere and the time it takes to reach the sphere are sampled using exact probability distributions. The algorithm is terminated if the particle has traveled beyond a preset threshold to emulate wandering off to infinity. If the particle has not traveled beyond that threshold, the algorithm returns to Stage I.

III. Interact with absorbing trap. The particle is now on the absorbing trap. If the trap is fully absorbing, the particle gets absorbed, and the total amount of time the particle has spent in the domain is recorded, and the algorithm is terminated. If the trap is partially absorbing, the FPT to the disk whose radius is the distance to the trap boundary is sampled using an exact probability distribution. For that amount of time, the particle is interacting with a partially absorbing disk. Therefore, we sample the survival probability of the particle using the solution to a one-dimensional diffusion problem with a partially absorbing boundary condition. If the particle is sampled to be absorbed in that amount of time, the total time is recorded, and the algorithm is terminated. If the particle has survived that time, then it is propagated to a cylinder whose radius is equal to the particle's distance to the trap boundary and whose height is drawn from an exact probability distribution. The

time taken by the particle is then recorded, and the algorithm returns to Stage I.

The details of the algorithms and the exact distributions used are given in the Appendices. The cumulative distributions in the algorithms are all precomputed before the algorithm starts running for a set of time and position values. Then we use the method of inverse transform sampling on the cumulative distributions for sampling times or positions. For inverse transform sampling, we use a binary search algorithm for computational efficiency.

V. CONCLUSIONS

In this paper, we studied the three-dimensional imperfect narrow escape problem for an arbitrary geometry with partially absorbing traps. Using the method of SLPT, we derived expressions for the leading-order asymptotic behavior of a Brownian particle's MFPT of exit in the limit of vanishing trap size for different absorption regimes. We used KMC algorithms to compute the capacitance values appearing in the analytical results and to numerically verify the analytical expression in a simple domain geometry (a rectangular prism with a single trap).

Our analysis yielded the following simple estimate of the MFPT for N identical, well-separated small traps, which is valid in any absorption regime,

$$v \approx \frac{|\Omega|}{4DNa}\left(1 + \frac{2}{K\pi}\frac{D}{a\tilde{\kappa}}\right), \tag{40}$$

where $K \approx 0.5854$. The estimate (40) resembles the following formula posited in [13] {see Eq. (57) in [13]} for a similar problem with a disk-shaped target on the boundary of the domain,

$$v \approx \frac{|\Omega|}{4DNa}\left(1 + \frac{4}{\pi}\frac{D}{a\tilde{\kappa}}\right). \tag{41}$$

Indeed, (40) differs from (41) only in the numerical prefactor of $2/(K\pi) \approx 1.09$ versus $4/\pi \approx 1.27$ in the second term. The greatest discrepancy between (40) and (41) is 17% and occurs in the low absorption regime of $a\tilde{\kappa}/D \ll 1$. Further, while (40) employed a heuristic estimate, this heuristic estimate is exact in the low-absorption regime of $a\tilde{\kappa}/D \ll 1$. We note that our simulation results in Fig. 1 agree with (40) rather than (41) [except in the high-absorption regime $a\tilde{\kappa}/D \gg 1$ in which (40) and (41) are equivalent].

The estimate (41) can be quickly derived using a recent and very general result of Chaigneau and Grebenkov [28]. For partially reactive targets located in the *interior* of the domain, these authors found the following MFPT estimate [28]:

$$v \approx \frac{|\Omega|}{DC}\left(1 + \frac{DC}{\kappa|\Gamma|}\right), \tag{42}$$

where $|\Gamma|$ is the surface area of the target and C is its harmonic capacity (defined such that the capacity of a sphere of radius a is $4\pi a$). If we take the target to be a one-sided disk of radius a, then $C = 4a$ and $|\Gamma| = \pi a^2$ and (42) yields (41). Although the estimate (42) was not claimed to be valid when the target is on the boundary {(42) was derived assuming that the target is far from the boundary [28]}, it is interesting that it is always within 17% of our estimate (40) for targets on the boundary.

Guérin *et al.* [12] recently investigated the imperfect narrow escape problem with a single trap and generated exact analytical asymptotic results in two-dimensional and three-dimensional domains in the limit of high confining volume and high absorption. Their asymptotic results provide higher-order correction terms to the leading-order term and reveal the dependence of the particle's initial distance from the trap.

The first-order asymptotic results for the MFPT of escape in this paper are applicable to domains of all shapes. The geometry of the domain, however, is important for the higher-order terms. One immediate extension of this paper is thus to compute the higher-order terms for the MFPT for different geometries using the specific Green's functions for that geometry [5].

The narrow escape scenario discussed in this paper could be modified to model more general biochemical scenarios. Diffusing proteins are known to exist in a number of conformational states with varying reactivity levels with ligands [29]. In order to capture the dynamic reactivity level of the proteins, one could change the assumption about the simple Robin-Neumann boundary conditions. The traps can be modeled to exhibit Markovian switching between different reactivity states. Similar problems of stochastic gating have been discussed in Refs. [30–34], and it would be interesting to extend the SLPT framework and the KMC algorithms used in this paper to account for such gating.

APPENDIX A: CAPACITANCE COMPUTATION FOR CASE 1 ($\kappa\varepsilon \gg 1$)

The KMC algorithm in this appendix simulates the problem described in (14). The algorithm implements the general method devised by Bernoff, Lindsay, and Schmidt [24]. Furthermore, the capacitance for this specific problem is known exactly and thus the simulations are not necessary. Nevertheless, we describe the algorithm to set up the exposition in the more complicated scenarios in the following appendices.

The domain is the infinite half-space, and the trap is a disk of radius $\alpha > 0$, which is perfectly absorbing. The algorithm leverages the fact that the solution to (14) has a probabilistic interpretation. In particular, $w_c(\mathbf{y})$ is the probability that a Brownian particle starting at $\mathbf{y}$ eventually hits the trap. To find an analytical expression for capacitance, we first define the $\overline{w_c}(\rho)$ to be the average of w_c over the surface of a hemisphere H of radius $\rho > \alpha$ centered at the origin, $H = \{(p, q, \eta) \in \mathbb{R}^3 : \sqrt{p^2 + q^2 + \eta^2} = \rho, \eta \geqslant 0\}$. Integrating the PDE in (14) over the surface of the hemisphere H, using the divergence theorem and that $\partial_\eta w_c = 0$ for $\rho > 1$ and $\eta = 0$, we get

$$\iint_H \Delta w_c \, dS = \int_{\partial H} \boldsymbol{\nabla} w_c \cdot d\,\vec{r} = \int_{\partial H} \partial_\eta w_c \, dr = 0,$$

with ∂H denoting the boundary of H, $\partial H = \{(p, q, \eta) \in \mathbb{R}^3 : \sqrt{p^2 + q^2} = \rho^2, \eta = 0\}$. Because of the radial symmetry of

$\overline{w_c}$, we can drop the angular derivatives in the Laplacian Δw_c in the above integral. We then interchange the integration and differentiation and use the definition of $\overline{w_c}(\rho)$ to rewrite the surface integral as

$$0 = \iint_H \Delta w_c \, dS = \left(\frac{2}{\rho}\partial_\rho + \partial_\rho^2\right)\overline{w_c}(\rho).$$

Using the far-field condition in (16), the solution to this differential equation satisfies

$$\overline{w_c}(\rho) = \frac{c_1(\alpha_n)}{\rho}, \quad \rho > 1.$$

We can therefore use KMC simulations to numerically estimate $\overline{w_c}(\rho)$ and scale it with ρ to compute $c_1(\alpha)$. For convenience, we choose $\rho = \alpha = 1$ in our simulations; thus Stage I initializes the particle uniformly on a hemisphere of unit radius. The particle starts in the bulk, and its position is $[p_0 \quad q_0 \quad \eta_0]^\top$, where $\eta_0 > 0$. The cumulative distribution for the time the particle takes to reach the plane $\eta = 0$ in Stage I is computed via [35]

$$t_{\text{to plane}} = \frac{1}{4}\left(\frac{\eta_0}{\text{erfc}^{-1}(U)}\right)^2, \qquad \text{(A1)}$$

where U is a uniformly distributed random variable on [0, 1]. Then the propagation in Stage I can be described by the mapping

$$\begin{bmatrix} p \\ q \\ \eta \end{bmatrix} \to \begin{bmatrix} p + \xi_1\sqrt{2t_{\text{to plane}}} \\ q + \xi_2\sqrt{2t_{\text{to plane}}} \\ 0 \end{bmatrix}, \qquad \text{(A2)}$$

where ξ_1, ξ_2 are independent, standard normal random variables.

The algorithm now checks whether the particle lands inside or outside the trap. If the particle lands inside the trap, then the algorithm moves to Stage III. The particle, thus, immediately gets absorbed, so the algorithm terminates and the absorption boolean is recorded as true. If the particle lands outside the trap, then the algorithm moves to Stage II, and the particle is propagated to a hemisphere whose radius is the particle's distance from the trap. The propagation in Stage II can be described by the mapping

$$\begin{bmatrix} p \\ q \\ 0 \end{bmatrix} \to \begin{bmatrix} p \\ q \\ 0 \end{bmatrix} + r\begin{bmatrix} \xi_1/\sqrt{\xi_1^2 + \xi_2^2 + \xi_3^2} \\ \xi_2/\sqrt{\xi_1^2 + \xi_2^2 + \xi_3^2} \\ \xi_3/\sqrt{\xi_1^2 + \xi_2^2 + \xi_3^2} \end{bmatrix}, \qquad \text{(A3)}$$

where $r = (\|[p, q, 0]^\top\| - \alpha)$ is the distance to the trap boundary, α is the radius of the trap in the inner problem, and ξ_1, ξ_2, ξ_3 are standard normal random variables.

The particle's distance away from the origin is then checked to see if the particle traveled beyond a threshold r_∞ (we set $r_\infty = 10^{10}$ in our simulations). If the particle has not traveled beyond that threshold, the algorithm returns to Stage I. If the particle has traveled beyond that threshold, we assume that it traveled to infinity. Therefore, the algorithm terminates, and the absorption Boolean is recorded as false. We notet that the probability of a particle starting at a distance r_∞ from

the trap being absorbed is on the order of $1/r_\infty$. Thus, our assumption that particles reaching this threshold never hit the trap introduces an error on the order of $1/r_\infty = 10^{-10}$.

After the algorithm runs for many trials, the capacitance value is computed by finding the ratio of trials in which the particle gets absorbed to the total number of trials.

APPENDIX B: CAPACITANCE COMPUTATION FOR CASE 2 ($\kappa\varepsilon = O(1)$)

The KMC algorithm in this appendix simulates the problem described in (23), again using that the solution $w_c(\mathbf{y})$ to (23) is the probability that a Brownian particle starting from $\mathbf{y}$ eventually gets absorbed at the partially absorbing trap. The domain is the infinite half-space, and the trap is a partially absorbing disk of radius $\alpha > 0$. In contrast to the previous apeendix, we are not aware of an exact formula for the capacitance of this problem and thus a simulation algorithm is necessary. The algorithm follows a method used in [19]. The analytical relationship between capacitance and average value of w_c over the surface of a hemisphere of radius $\rho > \alpha$ can be derived by following the steps in Appendix A,

$$\overline{w_c}(\rho) = \frac{c_2(\alpha, \varepsilon\kappa)}{\rho}.$$

Thus, we can similarly choose $\rho = 1$ and use KMC simulations to estimate $\overline{w_c}(1) = c_2(1, \varepsilon\kappa)$. The particle is similarly initialized uniformly on a hemisphere of radius 1. The Stage I and II propagations are exactly the same as the previous algorithm and we use the mappings in (A2) and (A3). We also similarly check if the particle traveled beyond $r_\infty = 10^{10}$. If so, we terminate the algorithm and set the absorption boolean equal to false.

If the particle gets mapped to the inside of the trap, then the algorithm moves to Stage III. Because the absorbing trap is not perfectly absorbing, the particle now is not immediately absorbed. We thus compute the distance to the trap boundary and scale the pre-computed cumulative distribution for the FPT to the unit disk with that distance. We then use inverse binary sampling to sample the time to reach the disk.

The precomputed cumulative distribution of the FPT to the unit disk is [36]

$$P_{\text{disk}}(\tau) = \sum_{r=1}^{\infty} \frac{2\exp\left(-q_r^2\tau/2\right)}{q_r J_1(q_r)}, \tag{B1}$$

where J_1 is the first-order Bessel function of the first kind and q_r are the ordered positive roots of J_0, the zero-order Bessel function of the first kind. Thus, for the particle at $[p_0, q_0, 0]^\top$, the time to reach a disk that touches the trap boundary is

$$t_{\text{to disk}} = (\|[p_0, q_0, 0]^\top\| - \alpha)^2 P_{\text{disk}}^{-1}(U) \tag{B2}$$

where U is uniformly distributed on [0, 1] and P_{disk}^{-1} denotes the inverse of (B1).

During this time $t_{\text{to disk}}$, the particle is necessarily above the partially absorbing boundary. Thus, this problem is described by a one-dimensional diffusion problem on the half-line with a partially absorbing boundary condition at 0 and a Dirac delta

function initial position,

$$\partial_t \rho = \partial_{\eta\eta}\rho, \quad \eta > 0,\, t > 0,$$
$$\partial_\eta \rho(0, t) = k\rho, \quad t > 0,$$
$$\rho(\eta, 0) = \delta(\eta), \quad \eta > 0,$$

where $\rho(\eta, t)$ is the particle density at position η and time t. The probability that the particle has not been absorbed by time t and is below height z is then

$$P_{\text{partial}}(t, z) = \int_0^z \rho(t, s)\, ds$$
$$= \text{erfcx}(k\sqrt{t}) - \exp\left(-\frac{z^2}{4t}\right)\text{erfcx}\left(\frac{z + 2tk}{2\sqrt{t}}\right),$$

where $\text{erfcx}(x) = \exp(x^2)(1 - \text{erf}(x))$.

We check if the particle is absorbed during time $t_{\text{to disk}}$ by checking if $U > P_{\text{partial}}(t_{\text{to disk}}, \infty)$, when U is uniformly distributed on [0, 1]. If the particle is absorbed, we terminate the algorithm, and the absorption boolean is recorded as true. If the particle is not absorbed, we sample the height of the particle by finding η_{next} such that

$$P_{\text{partial}}(t_{\text{to disk}}, \eta_{\text{next}}) = U.$$

Then, we use the following mapping to propagate the particle to the bulk:

$$\begin{bmatrix} p \\ q \\ 0 \end{bmatrix} \to \begin{bmatrix} p \\ q \\ 0 \end{bmatrix} + \begin{bmatrix} r\cos(2\pi\xi) \\ r\sin(2\pi\xi) \\ \eta_{\text{next}} \end{bmatrix}, \tag{B3}$$

where $r = (\alpha - \|[p, q, 0]^\top\|)$ is the distance to the trap boundary, α is the radius of the trap in the inner problem, and ξ is a random variable uniformly distributed over $[0, 2\pi]$.

After the particle is propagated, the particle's distance away from the origin is checked to see if the particle traveled beyond the preset threshold. If the particle has not traveled beyond that threshold, the algorithm returns to Stage I. If the particle has traveled beyond that threshold, we assume that it traveled to infinity. Therefore, the algorithm terminates and the absorption Boolean is recorded as false.

After the algorithm runs for many trials, the capacitance value is computed by finding the ratio of trials in which the particle gets absorbed to the total number of trials.

APPENDIX C: CAPACITANCE COMPUTATION FOR CASE 3 ($\kappa\varepsilon \ll 1$)

The KMC algorithm in this appendix simulates the problem described in (28). The domain is the infinite half-space, and the trap is reflecting. Unlike in the previous two algorithms, the solution $w_c(\mathbf{y})$ of (28) is the expected local time that a particle spends on the disk $\partial\Omega_A$ before it wanders off to infinity, conditioned that it starts at $\mathbf{y}$ [25].

To find the capacitance, the algorithm follows a method used in [19]. Similar to the previous two algorithms, we define $\overline{w_c}(\rho)$ to be the average of w_c over the surface of a hemisphere H or radius $\rho > \alpha$ centered at the origin, and we take $\alpha = 1$ without loss of generality. Following the steps in

Appendix A, we again obtain

$$\overline{w_c}(\rho) = \frac{c_3(1)}{\rho} = \frac{K}{\rho}, \quad \rho > 1,$$

for some constant K [the relation (29) then follows from a simple scaling argument]. We can, therefore, use KMC simulations to numerically estimate $\overline{w_c}(\rho)$ and scale it with ρ to compute K. We choose $\rho = 1$ in our simulations; thus Stage I initializes the particle uniformly on a hemisphere of radius 1. The Stage I and II propagations are exactly the same as the previous algorithm and we use the mappings in (A2) and (A3) for Stage I and Stage II, respectively. We also similarly check if the particle has traveled beyond a threshold value and terminate the algorithm if it did and record the accumulated local time. In Stage III, we compute $t_{\text{to disk}}$, the time the particle takes to reach a disk whose radius is the distance to the trap boundary, as discussed in Stage II and Eq. (B2). Before time $t_{\text{to disk}}$, the particle is necessarily above the trap and the problem is thus effectively one dimensional. The probability that the particle accumulates more than ℓ local time is then [37]

$$P_{\text{local}}(\ell) = 1 - \text{erf}\left(\frac{\ell}{2\sqrt{t_{\text{to disk}}}}\right),$$

and thus we can sample the change in local time as

$$\ell = 2\sqrt{t_{\text{to disk}}}\text{erf}^{-1}(U),$$

where U is uniformly distributed on [0, 1]. Conditioned on the change in local time ℓ, the probability that the particle is at height η at time $t_{\text{to disk}}$ is [37]

$$P_{\text{pos}}(\eta) = 1 - \exp\left(\frac{\ell^2 - (\eta + \ell)^2}{4t_{\text{to disk}}}\right).$$

We thus sample the new height of the particle as

$$\eta_{\text{next}} = \sqrt{\ell^2 - 4t_{\text{to disk}}\ln(1 - U)} - \ell$$

where U is uniformly distributed on [0, 1]. Then, we use the mapping in (B3) to propagate the particle to the bulk with r, α, ζ, ξ as defined in (B3).

After the particle is propagated, the particle's distance away from the origin is checked to see if the particle traveled beyond the preset threshold r_∞. If the particle has not traveled beyond that threshold, the algorithm returns to Stage I. If the particle has traveled beyond the threshold, we assume that the particle traveled to infinity. Therefore, the algorithm terminates, and the final value of the local time is recorded. After the algorithm runs for many trials, the capacitance value is calculated to be the average local time over these trials.

APPENDIX D: FULL SIMULATION

The KMC algorithm in this appendix simulates the problem described in (5). We take the domain to be a rectangular prism, defined by $\Omega = (-h, h) \times (-h, h) \times (0, L)$. We assume that there is only one partially absorbing trap

$\partial\Omega_\varepsilon = \{(x, y, 0) : x^2 + y^2 \leqslant \varepsilon^2\}$. The rest of the prism surface $\partial\Omega_R$ is reflective. In order to minimize the number of computations required in the algorithm, we exploit the radial symmetry of this problem. We periodically extend the domain and study the problem when the $z = 0$ plane has infinitely many partially absorbing traps placed on a square grid with grid size $2h$. This allows us to circumvent computing reflections from the sides of the prism as we can also always mod out the x, y positions of the particle by $2h$ to place the particle back in our original prism.

In this algorithm, the goal is to compute the total time the particle spends in the domain before it gets absorbed by the trap. Thus, we record the time the particle spends in each stage of the algorithm and compute the total sum of those times.

We initialize the particle uniformly in the prism domain. Then, Stage I similarly propagates the particle from the bulk to the plane. Since we now have a bounded domain, we cannot use the Stage I propagation formula in (A1) for $t_{\text{to plane}}$. We describe the problem as a 1D survival probability problem on the bounded domain $[0, 2L]$, where both ends of the domain are perfectly absorbing. This problem is studied in [38], and we precompute the given analytical solution on the $[0, L]$ domain. The problem and the solution are described by

$$\partial_t S_t = \partial_{zz}S, \quad 0 < z < 2L, t \geqslant 0$$
$$S(0, t) = 0, \quad t \geqslant 0$$
$$S(2L, t) = 0, \quad t \geqslant 0$$
$$S(z, 0) = 1, \quad 0 < z < 2L$$

$$S(z, t) = 1 - \begin{cases} \dfrac{\sum_{k=1}^{\infty}\left(1 - e^{-k^2\pi^2\frac{Dt}{L^2}}\right)\frac{2}{k\pi}\sin(k\pi\frac{z}{L})}{+\left(1 - e^{-k^2\pi^2\frac{Dt}{L^2}}\right)\frac{2}{k\pi}\sin\left(k\pi\left(1 - \frac{z}{L}\right)\right)} \\[2em] \overline{\sum_{k=-\infty}^{\infty}\text{sgn}(2k + \frac{z}{L})\text{erfc}\left(\frac{|2k + \frac{z}{L}|}{\sqrt{4\frac{Dt}{L^2}}}\right)} \\[1em] +\text{sgn}(2k + (1 - \frac{z}{L}))\text{erfc}\left(\frac{|2k + (1 - \frac{z}{L})|}{\sqrt{4\frac{Dt}{L^2}}}\right) \end{cases}$$

where the first sum converges fast for large t and the second one converges fast for small t. Before the algorithm is run, this cumulative distribution for the survival probability is precomputed for a set of t, z values, and the two formulas above are used for the $0 < t < 1$ and $t \geqslant 1$ regimes. We then pick the S values for which $0 \leqslant z \leqslant L$ since this survival probability problem was solved on the $0 \leqslant z \leqslant 2L$ domain. We then sample a time from this distribution by the equation

$$t_{\text{to plane}} = S^{-1}(U)$$

where U is uniformly distributed on [0, 1]. Then we use the mapping in (A2) to propagate the particle to the $z = 0$ plane. As there is no guarantee that this mapping would not place the particle outside the prism, we use the following mapping to make sure that the particle stays inside the prism defined by

$(-h, h) \times (-h, h) \times (0, L)$:

$$[p, q, z]^\top \rightarrow [\mathrm{mod}(p, 2h), \mathrm{mod}(q, 2h), z]^\top \quad \text{(D1)}$$

where $\mathrm{mod}(a, b)$ is defined as the modulo operation: $\mathrm{mod}(a, b) = a - b(\mathrm{floor}(b/a))$. $t_{\text{to plane}}$ value is recorded and depending on the particle's new position with the mapping in (D1), the algorithm either moves on to Stage II if the particle is outside the trap or to Stage III if the particle is inside the trap.

Stage II mapping is the same as the one described in the previous algorithm, but now we also compute the time for the particle to diffuse to the hemisphere as we want to record the time for each step. The MFPT to a sphere of radius R is a well-characterized problem and it has the following cumulative distribution [35]:

$$P(t, R) = \begin{cases} 1 + 2 \sum_{n=1}^\infty (-1)^n \exp\left(\frac{-n^2 \pi^2 t}{R^2}\right) \\ 2R \frac{1}{\sqrt{\pi t}} \sum_{n=0}^\infty \exp\left(-\frac{R^2(n+\frac{1}{2})^2}{t}\right) \end{cases}$$

where the first sum converges fast for large t and the second converges fast for small t. Before the algorithm is run, this cumulative distribution is computed for a set of t values and the two formulas above are used for $0 < t < 1$ and $t \geqslant 1$ regimes. We sample a time from this distribution by the equation

$$t_{\text{to hemisphere}} = (\|[p, q, 0]^\top\| - \alpha)^2 P^{-1}(U, 1)$$

where U is uniformly distributed on [0,1]. $t_{\text{to hemisphere}}$ is then recorded and the particle is placed uniformly on the hemisphere using the mapping in (A3) and ensured to be inside the prism by the modulo mapping in (D1).

In Stage III, as we have done in the previous algorithm, we compute the time $t_{\text{to disk}}$ by the formula in (B2). During $t_{\text{to disk}}$, the particle only sees the partially absorbing boundary at one end and the reflective boundary at the other end. Therefore, we can model the particle's behavior as a 1D diffusion problem on a bounded domain with a delta-function initial density,

$$\partial_t \rho = \partial_{zz} \rho, \quad 0 < z < L, t \geqslant 0$$
$$\rho_z(0, t) = 0, \quad t \geqslant 0$$
$$\rho_z(L, t) = -\kappa \rho, \quad t \geqslant 0$$
$$\rho(z, 0) = \delta(z), \quad 0 \leqslant z \leqslant L \quad \text{(D2)}$$

where $\rho(z, t)$ is the particle's density at position z and time t.

The solution to this problem can be computed via separation of variables, and the cumulative distribution for the survival probability of the particle can be found by integrating the solution with respect to z,

$$S(z, t) = \int_0^z \rho(s, t)\, ds$$
$$= \sum_{n=1}^\infty \frac{4 \cos(\mu_n L)}{2\mu_n L + \sin(2\mu_n L)} \exp\left(-\mu_n^2 t\right) \sin(\mu_n z)$$

where $\{\mu_n\}_{n=1}^\infty$ satisfies the transcendental equation $\tan(\mu_n L) = \frac{\kappa}{\mu_n}$.

We now check if the particle has been absorbed or not by checking if $U > S(L, t)$ where U is uniformly distributed on [0,1]. If $U > S(L, t)$, then the particle has been absorbed, so we sum the times the particle spent in different stages of the algorithm and record that total time. If $U \leqslant S(L, t)$, then the particle has not been absorbed, so we sample a z position at time $t_{\text{to disk}}$,

$$z_{\text{next}} = L - S^{-1}(U, t_{\text{to disk}})$$

where S^{-1} is the inverse of S with respect to z. Notice we are subtracting the sampled position from L to account for the fact that we modeled the reflective boundary to be at 0 and the partially absorbing boundary at L in (D2), while our problem has the boundaries flipped. We then use the mapping in (B3) with $\eta_{\text{next}} = z_{\text{next}}$ to propagate the particle to a new position and then use the modulo mapping in (D1) to make sure that the particle is inside the prism domain. The algorithm now returns to Stage I.

After the algorithm runs for many trials, the MFPT is computed to be the average FPT of these trials.

[1] J. W. S. Rayleigh, *The Theory of Sound*, Vol. 2, 2nd ed. (Dover, New York, 1945).

[2] P. C. Bressloff and J. M. Newby, Stochastic models of intracellular transport, Rev. Mod. Phys. **85**, 135 (2013).

[3] D. Holcman and Z. Schuss, The narrow escape problem, SIAM Rev. **56**, 213 (2014).

[4] Z. Schuss, A. Singer, and D. Holcman, The narrow escape problem for diffusion in cellular microdomains, Proc. Natl. Acad. Sci. USA **104**, 16098 (2007).

[5] A. F. Cheviakov, M. J. Ward, and R. Straube, An asymptotic analysis of the mean first passage time for narrow escape problems: Part II: The sphere, Multiscale Model. Simul. **8**, 836 (2010).

[6] S. Pillay, M. J. Ward, A. Peirce, and T. Kolokolnikov, An asymptotic analysis of the mean first passage time for narrow escape problems: Part I: Two-dimensional domains, Multiscale Model. Simul. **8**, 803 (2010).

[7] A. F. Cheviakov and M. J. Ward, Optimizing the principal eigenvalue of the Laplacian in a sphere with interior traps, Math. Comput. Modell. **53**, 1394 (2011).

[8] A. F. Cheviakov, A. S. Reimer, and M. J. Ward, Mathematical modeling and numerical computation of narrow escape problems, Phys. Rev. E **85**, 021131 (2012).

[9] F. Piazza, The physics of boundary conditions in reaction-diffusion problems, J. Chem. Phys. **157**, 234110 (2022).

[10] O. G. Berg and P. H. Von Hippel, Diffusion-controlled macromolecular interactions, Annu. Rev. Biophys. Biophys. Chem. **14**, 131 (1985).

[11] D. Shoup and A. Szabo, Role of diffusion in ligand binding to macromolecules and cell-bound receptors, Biophys. J. **40**, 33 (1982).

[12] T. Guérin, M. Dolgushev, O. Bénichou, and R. Voituriez, Imperfect narrow escape problem, Phys. Rev. E **107**, 034134 (2023).

[13] J. Reingruber, E. Abad, and D. Holcman, Narrow escape time to a structured target located on the boundary of a microdomain, J. Chem. Phys. **130**, 094909 (2009).

[14] D. S. Grebenkov, R. Metzler, and G. Oshanin, Effects of the target aspect ratio and intrinsic reactivity onto diffusive search in bounded domains, New J. Phys. **19**, 103025 (2017).

[15] D. S. Grebenkov and G. Oshanin, Diffusive escape through a narrow opening: New insights into a classic problem, Phys. Chem. Chem. Phys. **19**, 2723 (2017).

[16] D. S. Grebenkov, R. Metzler, and G. Oshanin, Towards a full quantitative description of single-molecule reaction kinetics in biological cells, Phys. Chem. Chem. Phys. **20**, 16393 (2018).

[17] D. S. Grebenkov, R. Metzler, and G. Oshanin, Full distribution of first exit times in the narrow escape problem, New J. Phys. **21**, 122001 (2019).

[18] A. M. Berezhkovskii, Y. A. Makhnovskii, M. I. Monine, V. Y. Zitserman, and S. Y. Shvartsman, Boundary homogenization for trapping by patchy surfaces, J. Chem. Phys. **121**, 11390 (2004).

[19] C. E. Plunkett and S. D. Lawley, Boundary homogenization for partially reactive patches, Multiscale Model. Simul. **22**, 784 (2024).

[20] D. S. Grebenkov, Paradigm shift in diffusion-mediated surface phenomena, Phys. Rev. Lett. **125**, 078102 (2020).

[21] D. S. Grebenkov, Diffusion-controlled reactions: An overview, Molecules **28**, 7570 (2023).

[22] M. J. Ward and J. B. Keller, Strong localized perturbations of eigenvalue problems, SIAM J. Appl. Math. **53**, 770 (1993).

[23] M. J. Ward, W. D. Henshaw, and J. B. Keller, Summing logarithmic expansions for singularly perturbed eigenvalue problems, SIAM J. Appl. Math. **53**, 799 (1993).

[24] A. J. Bernoff, A. E. Lindsay, and D. D. Schmidt, Boundary homogenization and capture time distributions of semipermeable membranes with periodic patterns of reactive sites, Multiscale Model. Simul. **16**, 1411 (2018).

[25] D. S. Grebenkov, Partially reflected Brownian motion: A stochastic approach to transport phenomena, in *Focus on Probability Theory*, edited by L. R. Velle (Nova Science Publishers, Hauppauge, NY, 2006), pp. 135–169.

[26] V. I. Fabrikant, *Applications of Potential Theory in Mechanics: A Selection of New Results*, Mathematics and its applications, (Kluwer Academic Publishers, Dordrecht, 1989).

[27] M. E. Muller, Some continuous Monte Carlo methods for the Dirichlet problem, Ann. Math. Stat. **27**, 569 (1956).

[28] A. Chaigneau and D. S. Grebenkov, First-passage times to anisotropic partially reactive targets, Phys. Rev. E **105**, 054146 (2022).

[29] D. Beece, L. Eisenstein, H. Frauenfelder, D. Good, M. C. Marden, L. Reinisch, A. H. Reynolds, L. B. Sorensen, and K. T. Yue, Solvent viscosity and protein dynamics, Biochemistry **19**, 5147 (1980).

[30] A. M. Berezhkovskii, D.-Y. Yang, S.-Y. Sheu, and S. H. Lin, Stochastic gating in diffusion-influenced ligand binding to proteins: Gated protein versus gated ligands, Phys. Rev. E **54**, 4462 (1996).

[31] Y. A. Makhnovskii, A. M. Berezhkovskii, S.-Y. Sheu, D.-Y. Yang, J. Kuo, and S. H. Lin, Stochastic gating influence on the kinetics of diffusion-limited reactions, J. Chem. Phys. **108**, 971 (1998).

[32] P. C. Bressloff and S. D. Lawley, Stochastically gated diffusion-limited reactions for a small target in a bounded domain, Phys. Rev. E **92**, 062117 (2015).

[33] S. D. Lawley and C. E. Miles, Diffusive search for diffusing targets with fluctuating diffusivity and gating, J. Nonlinear Sci. **29**, 2955 (2019).

[34] P. C. Bressloff and S. D. Lawley, Escape from subcellular domains with randomly switching boundaries, Multiscale Model. Simul. **13**, 1420 (2015).

[35] A. E. Lindsay, A. J. Bernoff, and M. J. Ward, First passage statistics for the capture of a Brownian particle by a structured spherical target with multiple surface traps, Multiscale Model. Simul. **15**, 74 (2017).

[36] Z. Ciesielski and S. J. Taylor, First passage times and sojourn times for Brownian motion in space and the exact Hausdorff measure of the sample path, Trans. Am. Math. Soc. **103**, 434 (1962).

[37] D. S. Grebenkov, Surface hopping propagator: An alternative approach to diffusion-influenced reactions, Phys. Rev. E **102**, 032125 (2020).

[38] S. Linn and S. D. Lawley, Extreme hitting probabilities for diffusion, J. Phys. A: Math. Theor. **55**, 345002 (2022).